TERRA AQUA ENVIRONMENTAL CONSULTANT LIMITED
Office Address: 1 Agunloye Street, 112104, Ota, Ogun State

Technical Report on Occurrence of Iron Mineralization around Owa-Onire, Sheet 224 Osi NW, Southwestern Nigeria

Submitted by

Ajadi, J. [1], Bankole, S. I.[2], Issa U.[1] and Jimoh, A. Y.[1]

[1]Department of Geology and Mineral Science, Kwara State University, Malete
[2]Department of Geology, University of Lagos, Lagos Nigeria.

1. Introduction

The reported iron deposit around Owa Onire is located within sheets 224 Osi NW topographic map and bounded by latitudes 8o19'30''N to 8o20'45''N and longitudes 5o05'15''E and 5o 09'15''E, covering about 200 cadastral units, and accessible from Oke Onigbin through Ora Road. A cursory geological spot check was carried out, involving sample grabbing which was analyzed to determine the economic potentials of the iron mineralization. Field observation revealed that the iron deposit around the study area is composed of ferruginous metasediments intercalating with quartzitic bands. The prospect investigation required sub-surface exploration through pitting and ground geophysical survey along with pre-defined profiles to obtain information on subsurface geology and possible mineralization thickness. Over 30 grab ore samples were obtained out of which Four (4) were selected for mineralogy, ore microscopy, and geochemical elemental composition analysis. This pre-feasibility study sought to generate an idea of the exploitability of the reported iron mineralization in the study area for the purpose of recommending the deposit for further detailed investigation. The surface geological observations were complemented by aeromagnetic data in order to establish regional structural trends, define lithological boundaries, and mineralization extent.

2. Local Geology

Traverses were carried out along and within some exposed areas of ironstone occurrence around Owa Onire community using available footpaths, river channels, surface drainage gullies, ridge tops, and break of slopes. Accessibility to rock outcrops for geological observations was achieved using a Germain GPS device, topographical base map, and Bruton compass, while fresh representative rock samples were obtained with the aid of an Eclogite sledgehammer. The Owa Onire Iron occurrence appeared to be a lateritic hardpan formed as a result of deep in situ weathering whose influence varies from 0.5m to 1.2m of depth as observed in the course of the traverses. The major rocks types observed

around the area are gneisses of the Precambrian Basement Complex rocks of Nigeria, which are unconformably overlain by the ferruginous quartzite of the older metasediment to the east and the micaceous to quarzitic schists of the younger metasediment to the west, which were indiscriminately intruded by the Older granite suites including granites and pegmatites which are capped by the lateritic soil of quaternary age. The granites occur mainly in association with the gneisses while some bosses and dykes of pegmatites intrudes the metasediments. Quartzite forms the prominent ridge of the historical "Kukuruku Hill" on top of which the popular Owu Water Falls emanates. An isolated body of decomposing quartzite ridge was observed NE of Owa Onire showing pervasive pegmatitic intrusions with evidence of the pneumatolytic hydrothermal fluid that possibly caused the pervasive but localized ferruginization of the quartzite in that locality. This is evident in the widespread occurrence of laterite outcrops sometimes with concentration and impregnation of the iron orebody on the hardpan peneplain to rolling topography (see appendices). There are also lateralized bodies of ferruginous quartzite as well as laterites derived from other rocks as a result of chemical weathering.

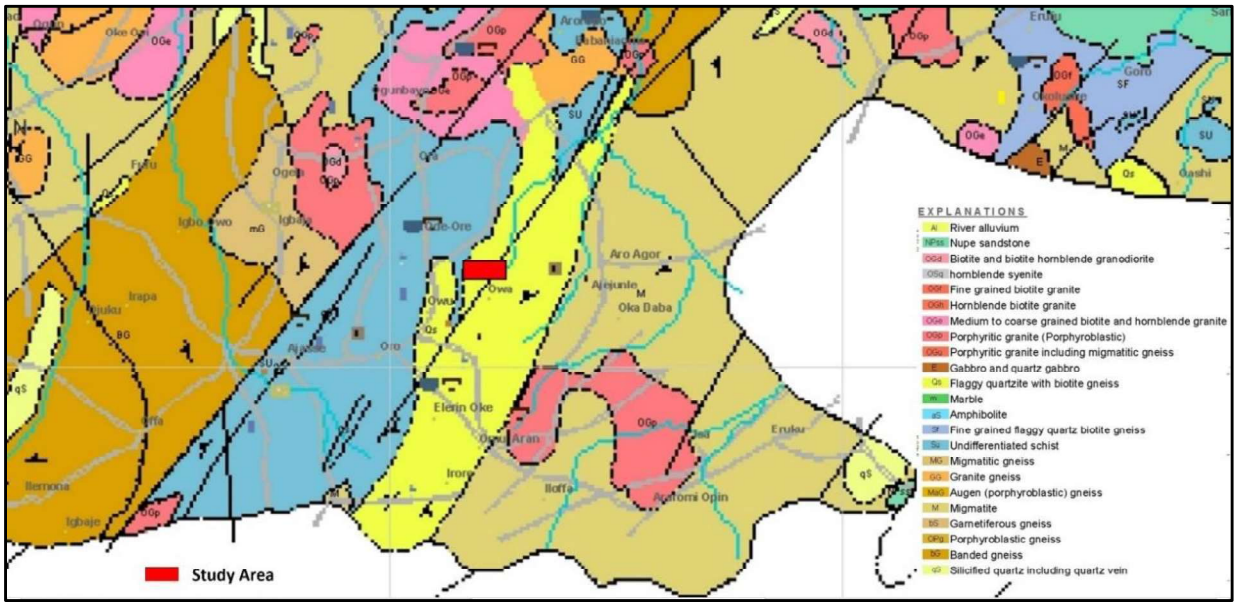


Figure 1: Geological map of Ilorin-Omuaran-Osi Areas showing the study location.

3. Mineralogy and Geochemistry

Four grab ore samples collected from the field were prepared and subjected to Xray Diffraction (XRD) analysis to determine their mineralogy which indicated iron mineral content ranging from hematite, ilmenite, siderite, and goethite. These are contained in sample 1 with hematite (12%), goethite (16%), and quartz (72%); sample 3 with ilmenite (18%), goethite (41%), and quartz (41%); sample 4A with siderite (27%), goethite (23%) and quartz (50%); and sample 4B with

100% goethite content (Figures 2, 3, 4, and 5). The four grab samples selected for laboratory studies were pulverized, prepared, digested, and analyzed using the X-ray Fluorescence (XRF) technique at the National Geoscience Laboratory of the Nigerian Geological Survey Agency (NGSA) at Kaduna which gave the percentage concentration of the following major element in these samples. The oxides include those of Fe2O3 (41.99% to 61.71%), SiO2 (3.1% to 18.49%), Al2O3 (3.80% to 11.40%), MgO (0.75% to 1.24%), TiO2 (0.23% to 1.05%) and SnO2 (0.22% to 1.21%). The result of the analysis expressed in percentage (%) of oxides is shown in Table 1 below. Both the composition of iron ore as indicated in Figures 2, 3, 4, and 5 from XRD analysis as well as the figures obtained from XRF analysis as contained in Table 1 suggest a low to medium iron ore grade which could be beneficiated for an enhanced grade.

Table 1: Elemental composition of oxides in the samples

SN	Oxide	Sample 1	Sample 3	Sample 4A	Sample 4B
1	Fe2O3	41.987	43.712	44.663	61.707
2	SiO2	18.493	13.902	13.437	3.104
3	Al2O3	11.404	7.169	5.480	3.799
4	MgO	1.24	0.91	0.75	0.79
5	P2O5	0.3119	0.5297	0.8270	2.2270
6	SO3	0.1427	0.0507	0.0467	0.1365
7	TiO2	1.051	0.623	0.4430	0.2831
8	MnO	0.1100	0.2411	0.2182	0.923
9	CaO	0.1130	0.0332	0.2653	0.958
10	K2O	0.0319	0.1104	0.0767	0.0247
11	CuO	0.00009	0.00099	0.00082	0.00101
12	ZnO	0.00130	0.00164	0.00188	0.01229
13	Cr2O3	0.0834	0.0259	0.0323	0
14	V2O5	0.2430	0.0906	0.0937	0.0904
15	As2O3	0.0149	0.0100	0.0100	0.0124
16	PbO	0.00068	0.00093	0	0.00089
17	Rb2O	0.000032	0.000050	0.000062	0
18	Ga2O3	0.00157	0.00083	0.00069	0.00016
19	NiO	0	0	0	0
20	Cl	0.072	0.028	0.055	0.117
21	ZrO2	0.1057	0.0117	0.0113	-0.02000
22	Ta2O5	0	0	0	0
23	WO3	0	0	0	0
24	Br	0.000087	0.000100	0.000094	0.000097
25	CeO2	0	0	0	0
26	ThO2	0	0	0	0
27	Y2O3	0.002049	0.002006	0.002018	0.002333
28	Nb2O5	-0.0200	-0.0300	-0.0300	-0.03000
29	I	0	0	0	0
30	BaO	0.016	0.045	0.0209	0
31	Ag2O	0	0	0.00051	0.00053
32	SnO2	1.210	1.212	0.215	0
33	U3O8	-0.050	-0	-0	-0.030
34	Bi2O3	0	0	0	0
35	GeO2	0.00036	0.00056	0.000506	0
36	Cs2O	0.00066	0	0.00037	0.00025
37	Sb2O3	-0.002	0.009	-0	-0.009
38	La2O3	0.31	0.73	0.91	0.901
39	CdO	0	0	0	0
40	Eu2O3	0.000343	0.000500	0.000473	0.001602
41	Gd2O3	0	0	0	0
42	Lu2O3	0.000056	0.000083	0.000097	0.000134
43	Co3O4	0	0	0	0

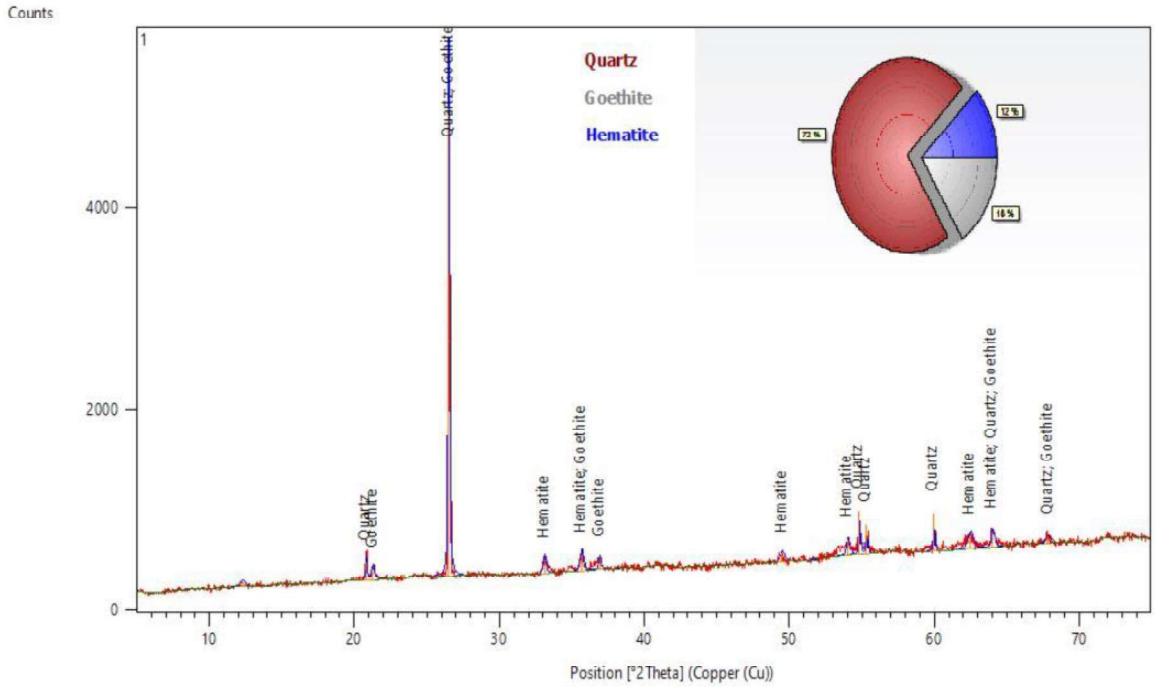


Figure 2: XRD analysis showing the mineralogy of sample 1.

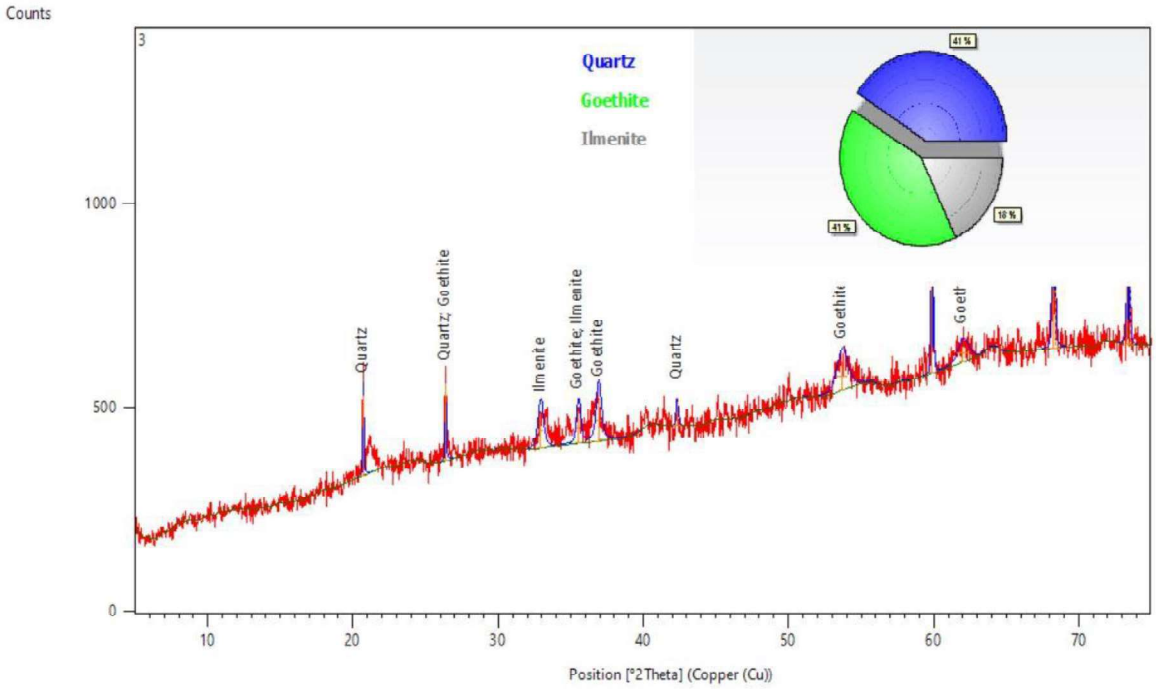


Figure 3: XRD analysis showing the mineralogy of sample 3.

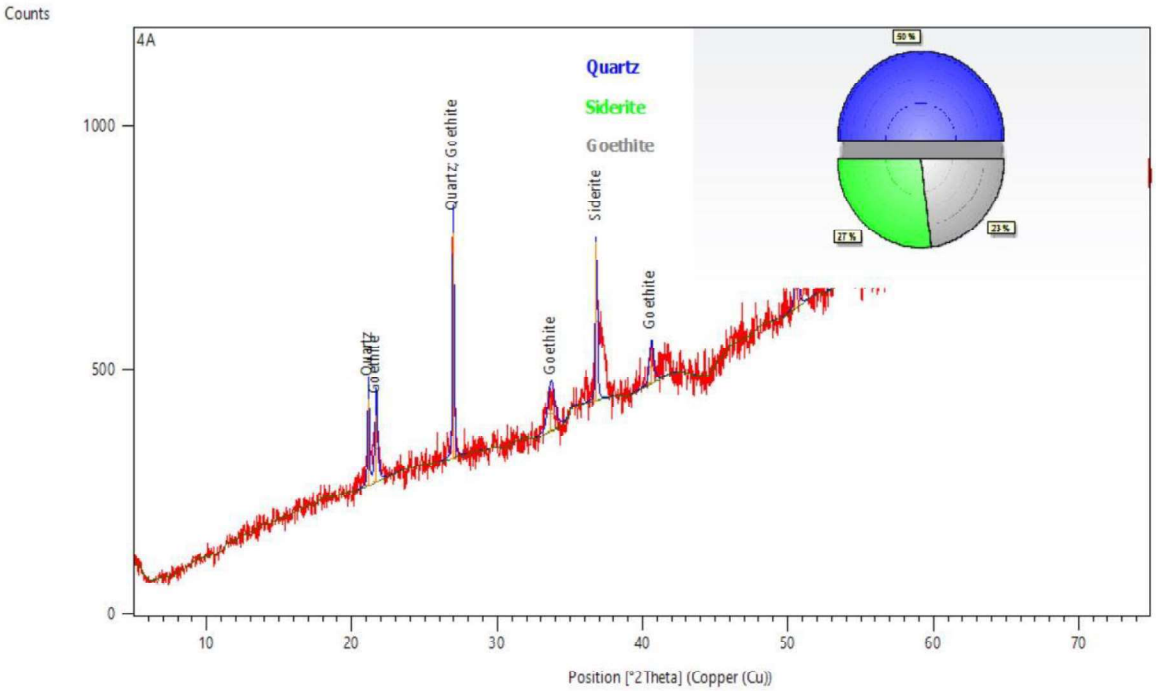


Figure 4: XRD analysis showing the mineralogy of sample 4A.

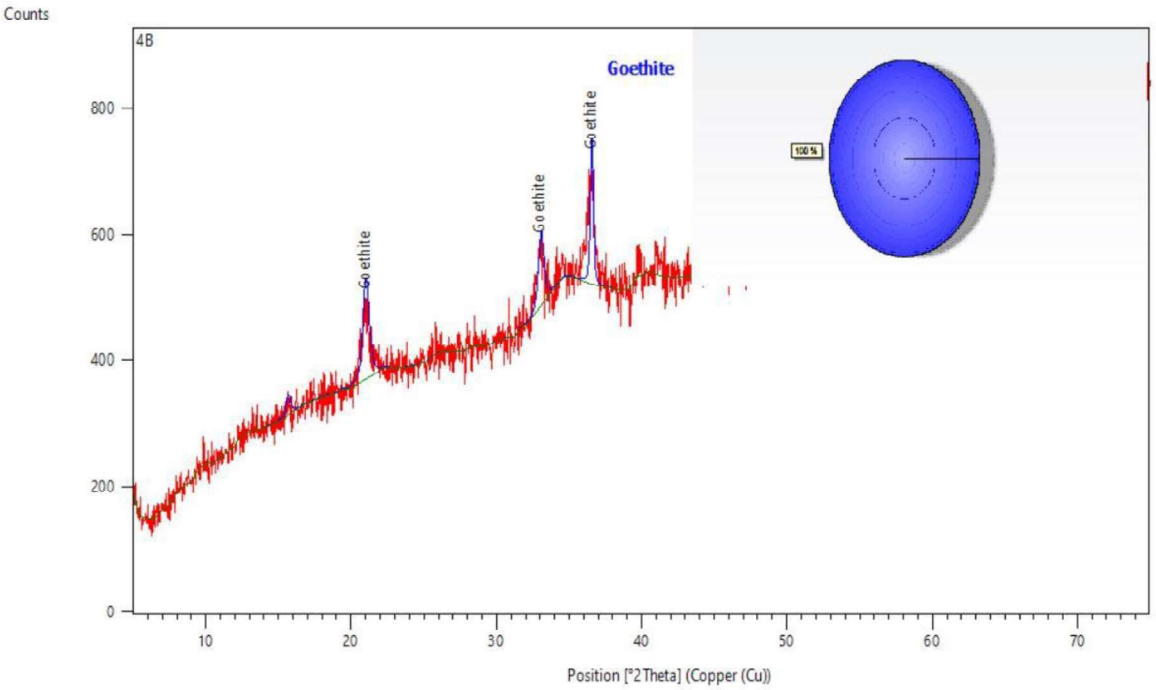


Figure 5: XRD analysis showing the mineralogy of sample 4B.

4. Geophysical Investigation

The magnetic measurement over the study area was taken using the aeromagnetic data obtained from the Nigerian Geological Survey Agency to delineate the probable mineralized areas for further intensive study to ascertain the viability of the deposit as an ore of economic importance by determining the ore grade and reserve. Aeromagnetic images of Total Field Magnetic Intensity (Figure 7), Residual Magnetic Intensity (Figure 8), Reduction to the Magnetic Equator (Figure 9), Tilt Derivative (TDR) Map (Figure 10), Analytic Signal Map (Figure 11), and First Vertical Derivative (Figure 12) were generated and interpreted.

4.1 Total Field Magnetic Intensity (TMI) Map

The total-field magnetic intensity (TMI) map (Figure 7) reveals three main types of total-field magnetic anomalies ranging in intensity from -23.11– 58.59nT that are depicted in red, pink, green, yellow and blue colour. The anomalies were classified into high, moderate and low amplitude anomalies. The high amplitude total-field magnetic anomalies associated with intensity between 29.81 to 50.61nT, which are shown in red and pink colours, occupied portion of the northern central part. Other areas of high amplitude include the western part and upper eastern part. The moderate amplitude magnetic anomalies values ranging from 11.38 to 29.81 nT, shown in yellow and green colour are widespread throughout the area. The prominent low amplitude anomalies ranging in intensity from -23.11 to 11.38 nT are shown in blue colour and are wide spread throughout the study area. Generally, the anomalies were depicted as short and high wavelength anomalies that are linear and circular in shape trending along NE- SW and NW- SE directions.

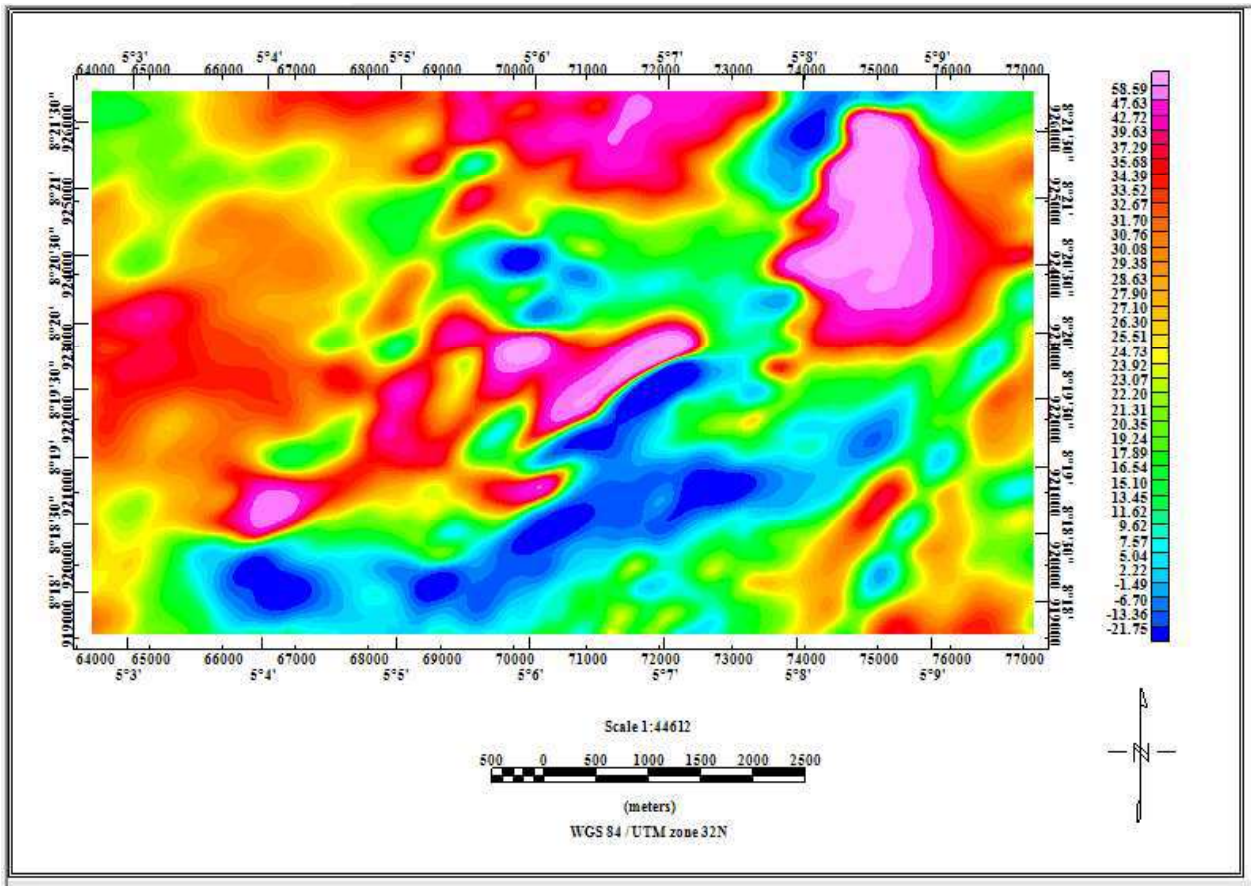


Figure 7: Total Magnetic Intensity (TMI) Map of the Study Area

4.2 Residual Magnetic Intensity (RMI) Map of the study area

Figure 8 shows the colour shaded map of the residual magnetic field intensity over the study area ranging from -36.69 to 28.84 nT and depicted in red, pink, yellow, green and blue colours. The positive residual intensities range from 0.59 to 28.84 nT with the high amplitudes ranging between 5.8 to 37.5 nT and depicted in red and pink colours. The negative residual intensities are ranging between -36.69 to -0.13 nT. The high positive amplitude anomalies are widespread throughout the study area and are dominant in the north-central part, the lower part of west and east directions and with less dominance which are widespread throughout the study area. Similarly, the negative amplitude anomalies are majorly found in the central part of the study area with dominance in the half southern region. However, high magnetization, usually associated with high positive residual amplitude suggests the presence of mafic to ultramafic rocks of high magnetic contents that are mineral potential targets as they often contain magnetic minerals such as magnetite and ilmenite. Low magnetization associated with negative residual intensities reflects either area of deep basement surface or areas containing minerals of low magnetic contents such as shale, silica, limestone and sandstone. The residual field anomalies were depicted in form of long and short-wavelength anomalies that are linear and circular in shape. The short-wavelength anomalies suggest near-surface

magnetized intrusions while the long wavelength suggests deep-seated bodies typical of areas associated with thick sediments. The long-wavelength anomalies are dominant in the northern, central and eastern parts of the study area while the low wavelength anomalies are dominant in the southern part of the study area. The general trends of these anomalies were observed to be along ENE-WSW, NE-SW and NW-SE directions.

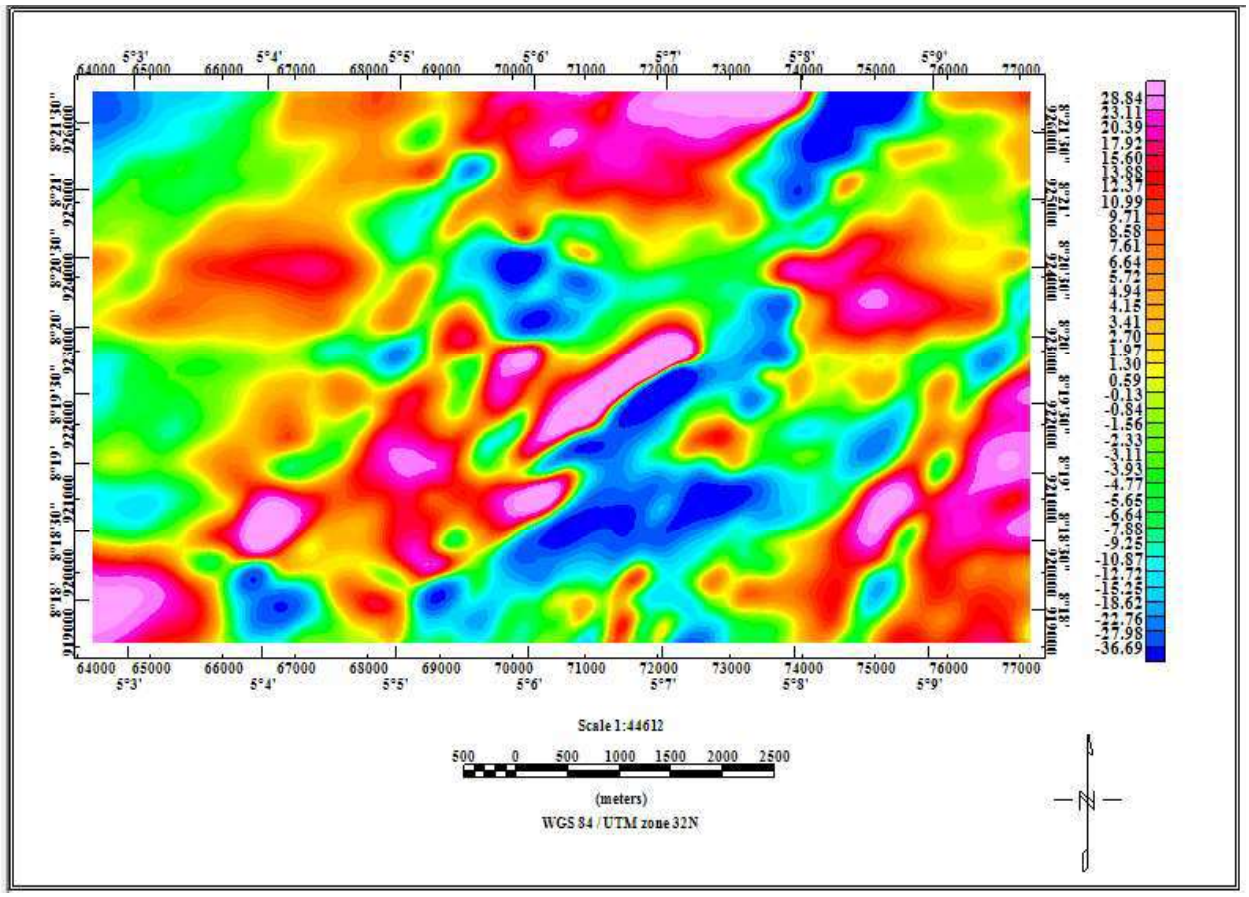


Figure 8: Residual Magnetic Field Map of the Study Area

4.3 Reduction to the Magnetic Equator (RTE)

The colour shaded map of the RTE residual magnetic field intensity (Figure 9) exhibit negative and positive values ranging from -21.75 to 50.61 nT shown in red, pink, yellow, green and blue colours. The positive RTE is broadly characterized by intensities ranging from 0.85 to 50.61 nT with the high amplitude ranging between 31.34 to 50.61 nT and depicted in red and pink colours. The intermediate positive value is shown in yellow colour with the range between 26.91 to 31.34 nT and the negative RTE intensities range between -23.11 to -3.35 nT depicted in blue colour. The shape of the anomalies on the RTE map are of short and long wavelength form and also circular and elongated in shape. The high prominent negative amplitude anomalies, shown in green colour, are dominant in the southern region while the very low amplitude

negative anomalies displayed in blue colour with circular and elongated shapes are dominant in the half northern region. Generally, the negative amplitude anomalies are circular and linear in shape trending along NE- SW and NW- SE directions, which is consistent with the trends of the TMI and RMI anomalies. A comparison between the RMI and RTE-TMI anomalies suggests a slight eastward shift of the RTE-RMI anomalies compared with the positions of the RMI anomalies.

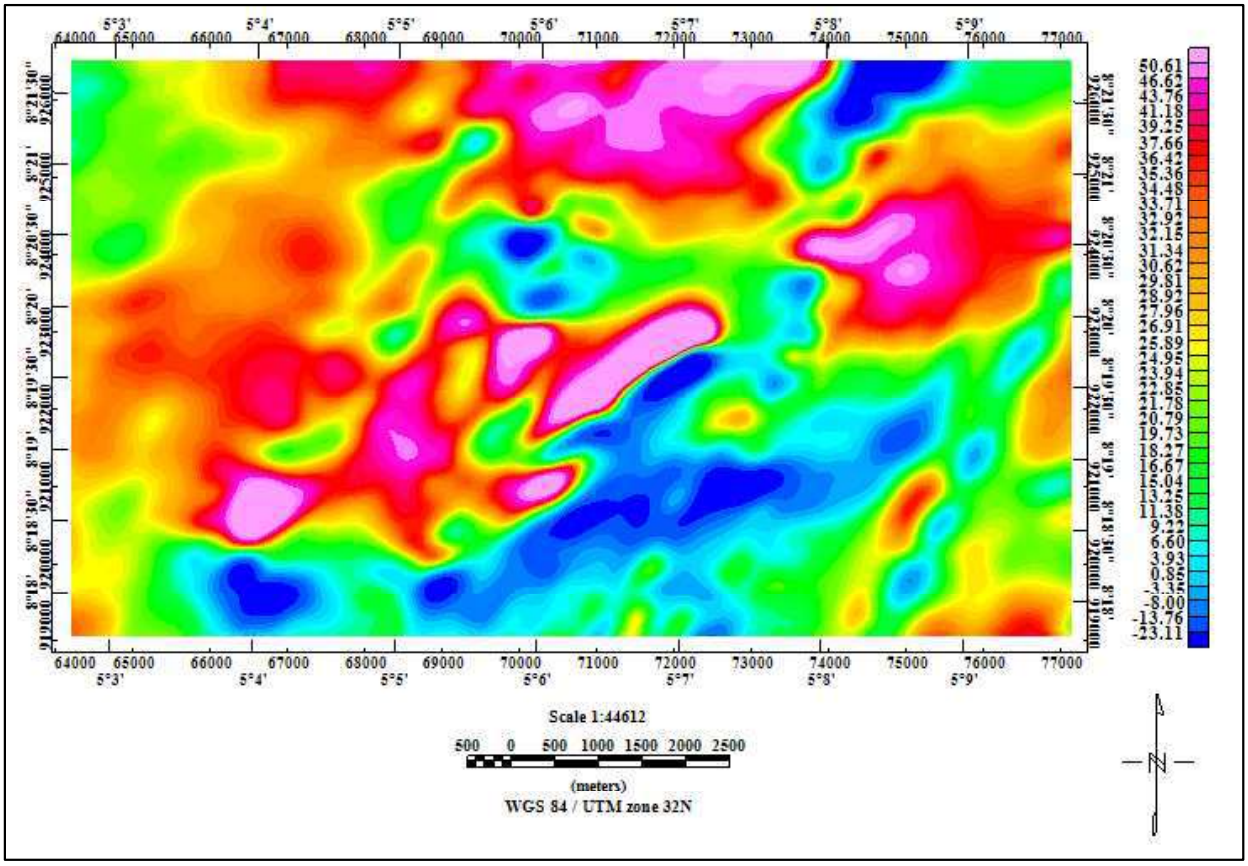


Figure 9: Reduction to the Equator Map of the Study Area

4.4 Tilt Derivative (TDR) Map

Figure 10 shows the wavelength anomalies that are circular and elliptical in shape ranging from -1.31635 to 1.36019 nT/m and depicted in pink, red, yellow, green and blue colour. The high positive gradient TDR anomalies which are prevalent throughout the study area depicted in pink and red colours. The intensities of these anomalies vary between 0.13720 to 1.36019 nT/m and are predominantly linear in shape. The low positive TDR values shown in yellow colour, ranges between 0.1372 to 0.5517 nT/m and are depicted as boundary separating the high positive and negative TDR gradient values. As the high positive gradient TDR values reflect magnetic sources,

the low positive TDR intensities which are close to zero, were interpreted to reflect geologic boundaries. The prevalence of high gradient positive TDR intensities suggests presence of subtle mafic to ultramafic rocks that are covered by the overlying sediments. Also, the negative gradient TDR anomalies shown in green and blue colour with intensities between -1.31635 to -0.020 nT/m occupy the study area and are linear and elliptical in shape.

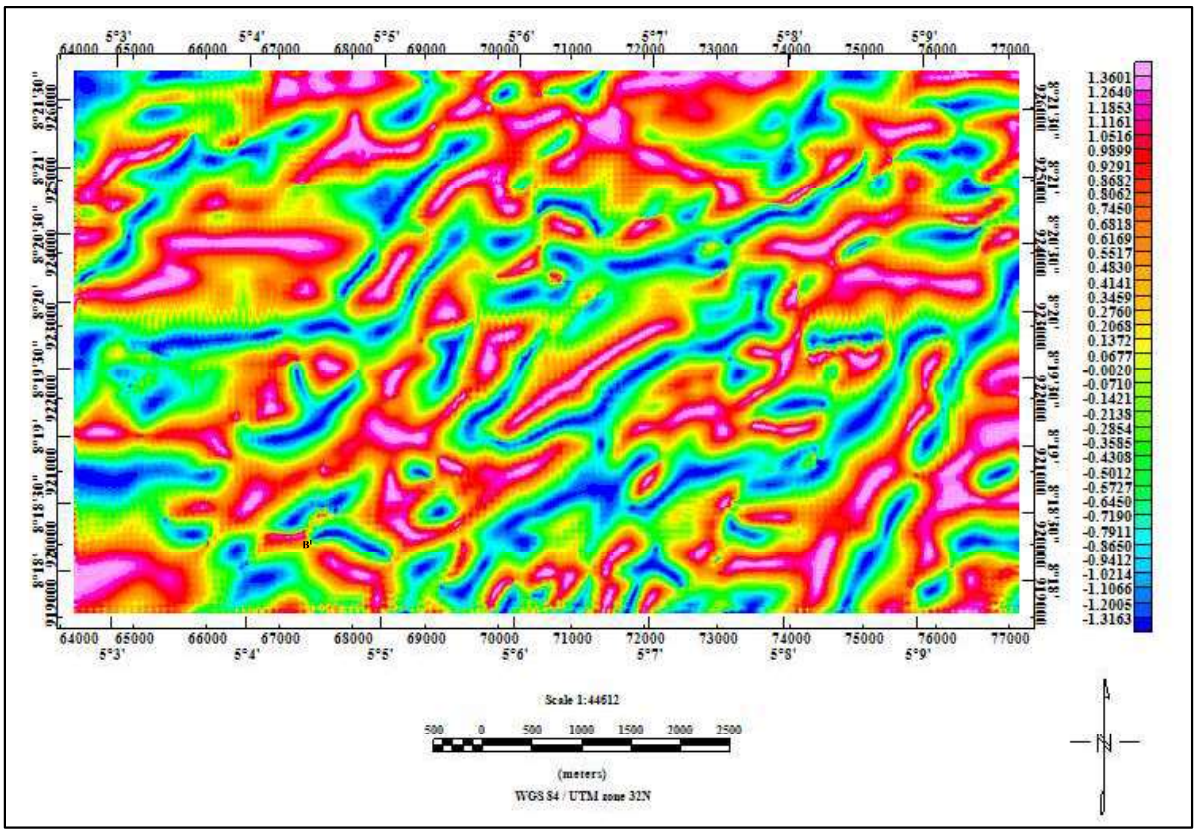


Figure 10: Tilt Angle Derivative Map of the Study Area

The low gradient negative TDR intensities are interpreted to reflect the presence of low magnetic content sediments such as limestone and sandstone in the area. The TDR anomalies identified in this area are trending along NE-SW, NW-SE, E-W and NNE-SSW direction. According to Onyedim *et al.,* (2009) the orientation of these lineaments along different directions suggests that the region between the major lineaments is occupied by the minor lineaments developed at different geologic phases.

4.5 Analytical Signal (AS)

The analytical signal amplitude was calculated upward continuation to see the distribution of the magnetic signature irrespective of the direction of the magnetization (i.e. locations of the magnetic

anomalies) in the study area. It simplifies the interpretation by placing the anomaly peaks directly above the source. It is independent of the direction of the magnetization of the source and is related to the amplitude of magnetization. The image from the map (Figure 10) divides the actual magnetic intensity anomalies zones into high and low magnetization. The regions of high amplitude magnetic signature ranging from 0.0514 to 0.2301 nT/km generally show a NE-SW trend clearer picture which is interpreted as faulted basement blocks having high magnetization. The low magnetic anomalies areas ranging from 0.0084 to 0.00514nT/km are clearly observed in the western and eastern parts of the map.

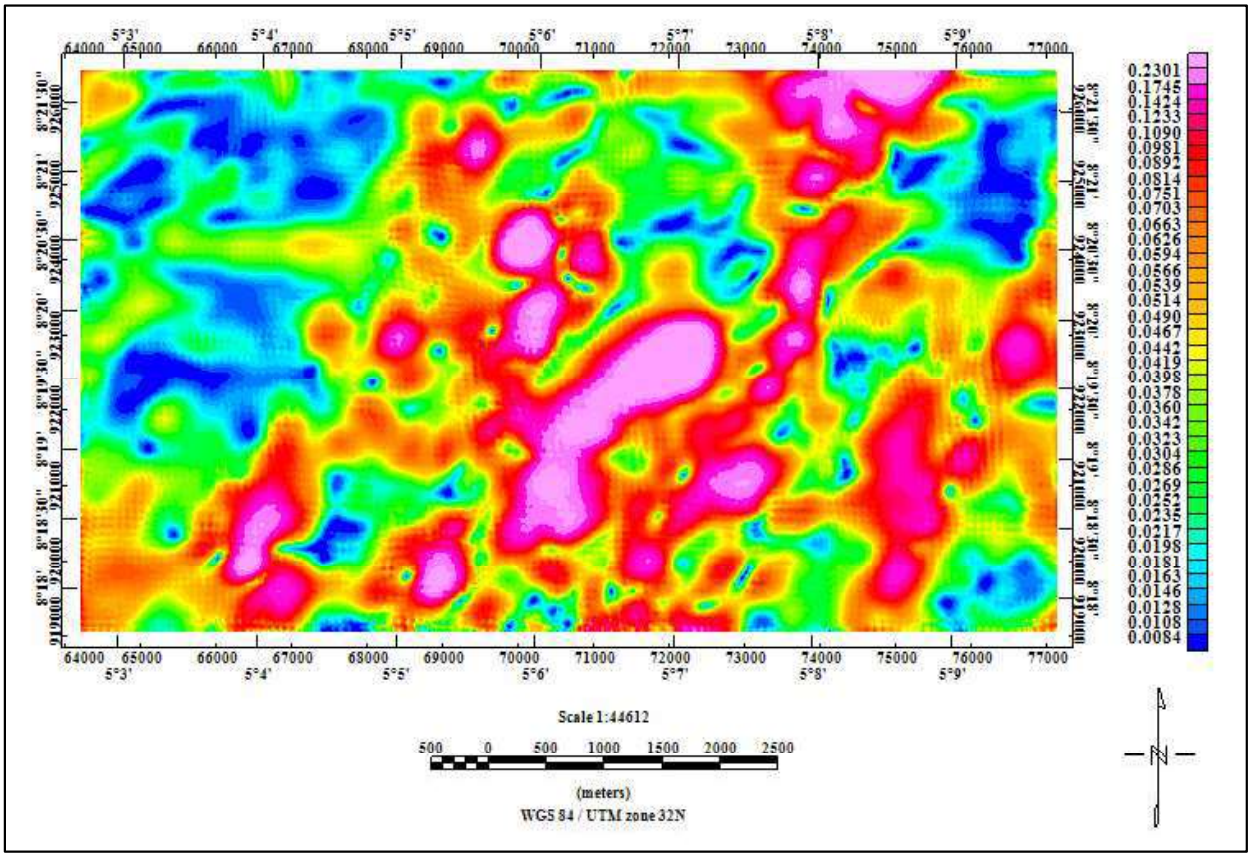


Figure 11: Analytic Signal Map of the Study Area

4.6 First Vertical Derivative (FVD)

The first vertical derivative map (Figure 12) shows different magnetic anomalies depicted in pink, red, yellow, blue and green colours characterized by positive and negative intensities ranging from -0.1216-0.0920 nT. The areas of higher positive intensity (high signal) ranging from 0.0051 - 0.0920 nT are widely spread out throughout the map of the study area. The widespread low negative intensity (low signal) ranging from -0.1216- -0.0016nT depicted in blue and green colour is also found in the study area. The map is also characterized by the wavelength anomalies of short

and long shape elliptical and several structural trends. The lineaments are trending majorly in the NE-SW while minorities are trending towards NW-SE directions. The shape of this structural lineament is also curve-linear spanning from the west part to the northeastern part of the area. The presence of high positive frequency indicates the presence of intrusive bodies which simply means that the region is tectonically active. The low negative magnetic susceptibility intensities could be a result of the presence of low magnetic contents such as limestone and sandstone in the area corresponding to low magnetic signatures.

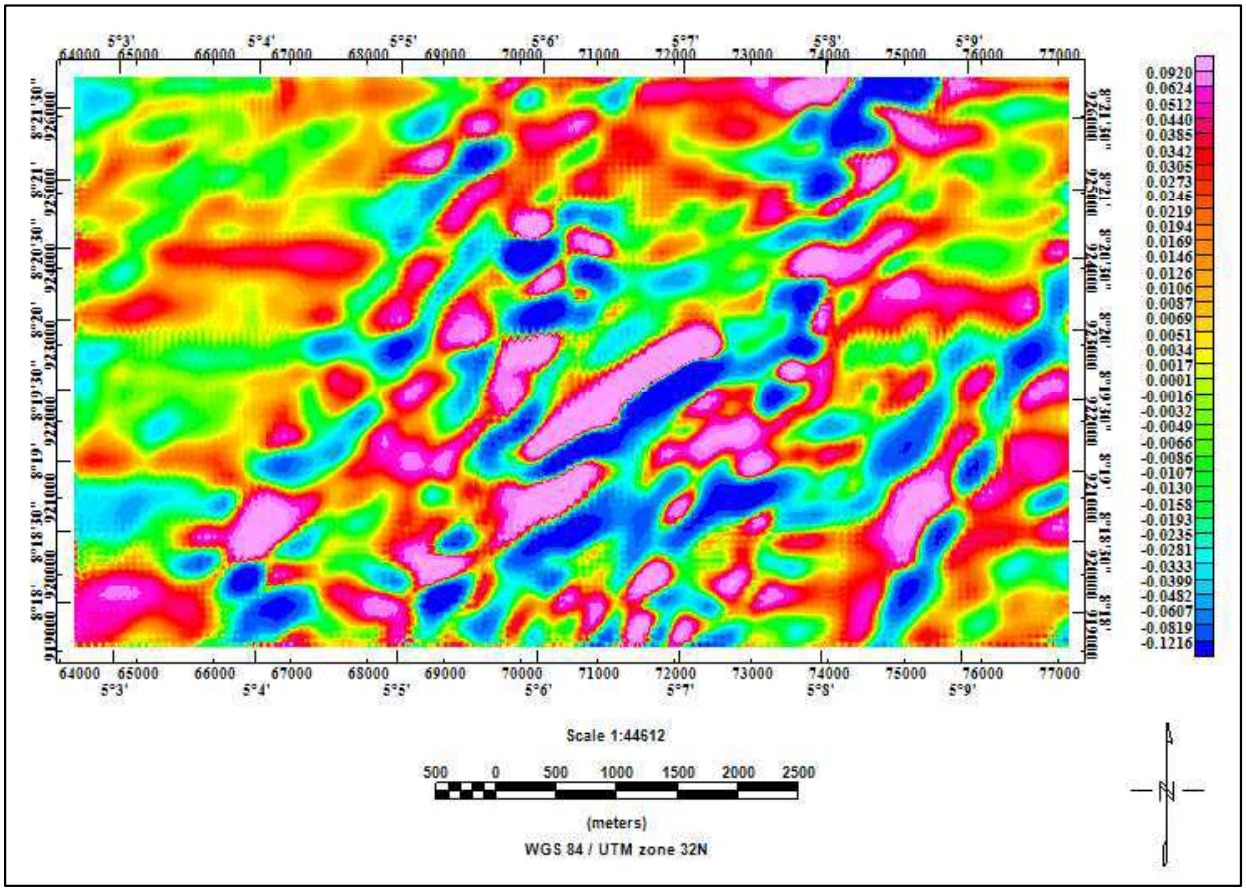


Figure 12: First Vertical Derivative Map of the Study Area

5.1 Conclusion

Reconnaissance geological sampling of the Owa Onire iron ore prospect on a scale of 1:25,000 was carried out to establish if the reported prospect is a mineralization show or an ore deposit as well as to ascertain its economic potential. Field observation and geophysical studies revealed that the prospect is extensive and its thickness and viability in terms of grade and reserve need to be determined for immediate exploitation. An old, abandoned trench revealed about 0.5m to 1.2m

thickness of lateritic iron ore. Personal communication with the inhabitants revealed that the old abandoned trench was dug in the past for iron production used for hunting, smelting and farming tools as the area was reputed as the home of iron in the ancient time. All these lend credence to the high possibility of having a good reserve of iron ore that could adequately support small to medium scale iron rod production if properly investigated.

References

Onyedim G., Alagoa K. D., Isaac Adedokun, Aderogba A. A., and Cyril Ovuru (2009): Mapping High-angle Basement Faults in the Middle Benue Trough, Nigeria from Gravity Inversion Surface. Earth Sciences Research Journal 13 (2): 140-147.

Appendices: Field Photographs








TOYOT
LRN 70AM